



Publication Year	2019
Acceptance in OA @INAF	2024-03-20T16:12:37Z
Title	The MAORY Science Operation activities
Authors	ARCIDIACONO, CARMELO; GULLIEUSZIK, MARCO; PORTALURI, ELISA; CANTIELLO, Michele; PAIANO, Simona; et al.
DOI	10.5281/zenodo.7711803
Handle	http://hdl.handle.net/20.500.12386/34995

The MAORY Science Operation activities

Carmelo Arcidiacono^{a,e*}, Marco Gullieuszik^a, Elisa Portaluri^{a,e}, Michele Cantiello^b, Simona Paiano^c, and Paolo Ciliegi^d

^aINAF-Osservatorio Astronomico di Padova, Vicolo dell'Osservatorio 5, 35122 Padova, Italy

^bINAF-Osservatorio Astronomico d'Abruzzo, Via Mentore Maggini snc, Loc. Collurania, 64100 Teramo, Italy

^cUniversità degli Studi dell'Insubria, Via Ravasi, 2, 21100 Varese, Italy

^dINAF - Osservatorio di Astrofisica e Scienza dello Spazio di Bologna, Via Piero Gobetti, 93/3, 40129 Bologna, Italy

^eADONI - Laboratorio Nazionale di Ottica Adattiva, Italy

ABSTRACT

The Preliminary Design Review of the MAORY, the MCAO module of the ESO ELT, is approaching. The collection of science cases in the white book was a major milestone for the team. The phase of verification of the scientific capabilities is currently ongoing. The verification of the feasibility of, at least, a few emblematic cases is mandatory to assess the current instrument baseline. The ultimate goal of the Science Operation Working Group is to define optimal strategies for the different MICADO/MAORY observing modes and to check performance in terms of astrometric and photometric precision and limits.

Keywords: Adaptive Optics, Extremely Large Telescope, Science Cases

1. INTRODUCTION, AREAS OF ACTIVITY

The "Science Operation" (SO) Working Group (WP) focuses the activity on the simulation of the Multi-conjugate Adaptive Optics Relay for the ELT (MAORY)¹ science cases,² deriving in this way the achievable performance in different observing conditions, as can be the case of a crowded globular cluster or an almost star-empty frame on high-*z* target. To produce as most as possible accurate simulations, we invest our efforts working on the many details that compose an observation, characterized for example by long exposure frames, different elevation values and therefore a rotating telescope pupil and a varying airmass. The group is entitled to generate the Point Spread Function (PSF)³ corresponding to the possible observations and to take into account the various effects that may be detrimental for the astrometric precision. The SO WP cooperates with the technical team in order to contribute to the solution of the trade-off presently ongoing on the design. SO WP offers what would be the user's point of view providing a further merit function to the solution. The SO WP task is complementary to the activities of the MAORY Science Team, that benefits of the relation with the technical group⁴ to assess the actual MAORY scientific potential.

2. PSF GENERATION AND ANALYSIS

The core business of SO WP is the generation of the PSF for both Single Conjugate Adaptive Optics (SCAO) and Multi-Conjugate Adaptive Optics^{5,6} (MCAO) cases. For the science user and operatively speaking the PSF offers a very compact representation of the MAORY results. The PSF is the essential ingredient to develop a scientific evaluation. The simulation of the PSF has to take into account also the characteristic introduced by the scientific instrument served by the MAORY module (filter, transmission, emissivity, WF error). To date, the only available option is the Multi-AO Imaging Camera for Deep Observations - MICADO,⁷ a second instrument is still to be defined. SCAO PSF making is the simplest case to simulate, since it does not depend on the Natural Guide Star (NGS) configuration in the way MCAO does. We generated the SCAO PSFs using the MAO

Further author information: (Send correspondence to C.A.)

Carmelo Arcidiacono.: E-mail: carmelo.arcidiacono@inaf.it, Telephone: 39 049 829 3414

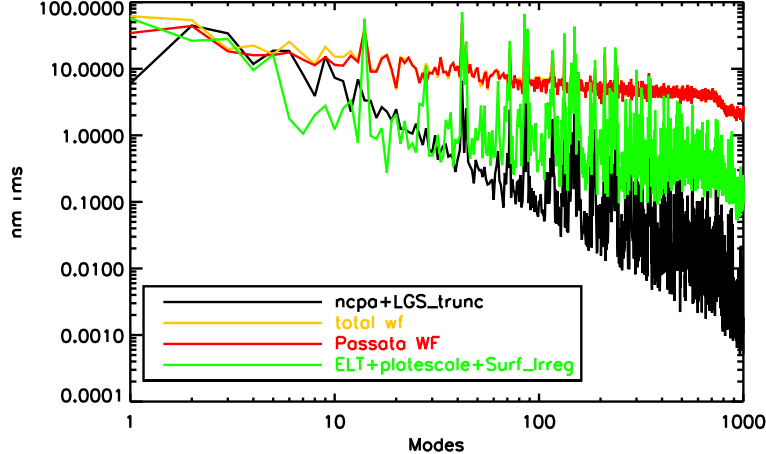


Figure 1. Here we plot the various spectral components that contribute to the residual WF used for the generation of MAORY PSF. The PASSATA residuals are computed considering six different turbulence realizations of 3.25 seconds each, as well as for NCPA and plate scale effects.

code⁸ considering the pyramid⁹ WFS and standard Armazones turbulence for a bright and mid-to-faint case of 15th NGS mag. For the results included in this paper, we consider an MCAO PSF set that originates from the combination of the PASSATA¹⁰ numerical simulation and WF error budget contribution digested using MAO. Using PASSATA we get the residual WF of the atmospheric disturbance. To this we added the WF error part that includes dynamical and static footprint of the telescope (M2 mid-spatial frequency, plate scale variation induced by M2 flexure) and a number of error sources originated within MAORY-MICADO (the Non Common Path Aberration (NCPA), Laser Guide Star (LGS) truncation error,¹¹ plus minor effects such as mid-spatial frequencies of the whole optical train). We combined six Monte Carlo¹² realizations to generate an average PSF model. For each run, PASSATA generates a bundle of independent phase screens, one for each turbulent layer. For our analysis, PASSATA was instructed to use the vertical profile of the statistical properties of the turbulence valid for the Cerro Armazones site. MAO produces or reads from file different realization of telescope aberrations eventually corrected by the MCAO loop and adds additional WF error representing NCPA and static uncorrected errors.

For each of the six simulations, we produce the evolution history of the WF corresponding to a number of stars over the MICADO FoV ($50''.4 \times 50''.4$). MAO computes the monochromatic PSF for 5 different wavelengths, equally spaced within each broadband filter considered (I, Y, J, H, Ks). Eventually, the PSF is integrated over the filter by summing about 50 monochromatic PSF and using a gray body emission model. Actually, SimCADO can use the monochromatic PSF to generate a final PSF integrated over the wavelength and considering the spectral profile of the source. We tested successfully this option.

To date, our ability to consider the spatially variant PSF is limited to a straightforward "jump" from one PSF region to the next. In this paper, we limited the analysis to a spatially constant PSF.

3. PHOTOMETRY AND COLOR DEPENDENCIES

Looking in to the plot in Figure 2 we see that within a broad band filter the Strehl Ratio (SR) can change significantly, especially for low values ($SR \lesssim 20\%$ typical of bluer wavelengths). Actually, blue and red stars can turn out having somewhat different PSF. For example, in J, SR varies by a factor of 2 within the filter: stars with different colors show slightly different PSF. Considering the J band, a circular aperture of radius= $\lambda/D = 6.6\text{mas}$ (λ is the wavelength and D is the diameter of the ELT), a star with J-K=0 appears 0.14 mag brighter, in that aperture, than a J-K=1 star, with identical integrated flux over the PSF area. The point here is that light spills out of the aperture according to the effective level of correction, which is a function of the wavelength. Similar considerations apply also for PSF fitting photometry: the modelization of the PSF depends on the wavelength. It is worth noting that many data analysis tools (i.e. Daophot¹³) use a field dependent PSF model derived from

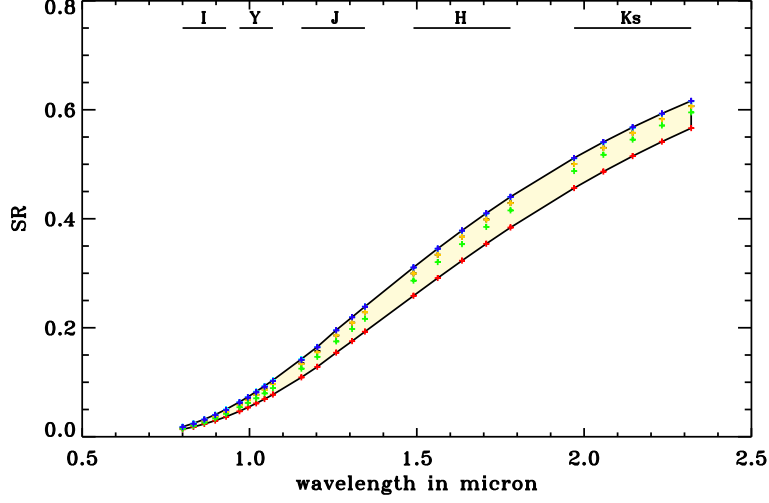


Figure 2. MCAO case: SR distribution over the 6 atmospheric and aberrations realizations.

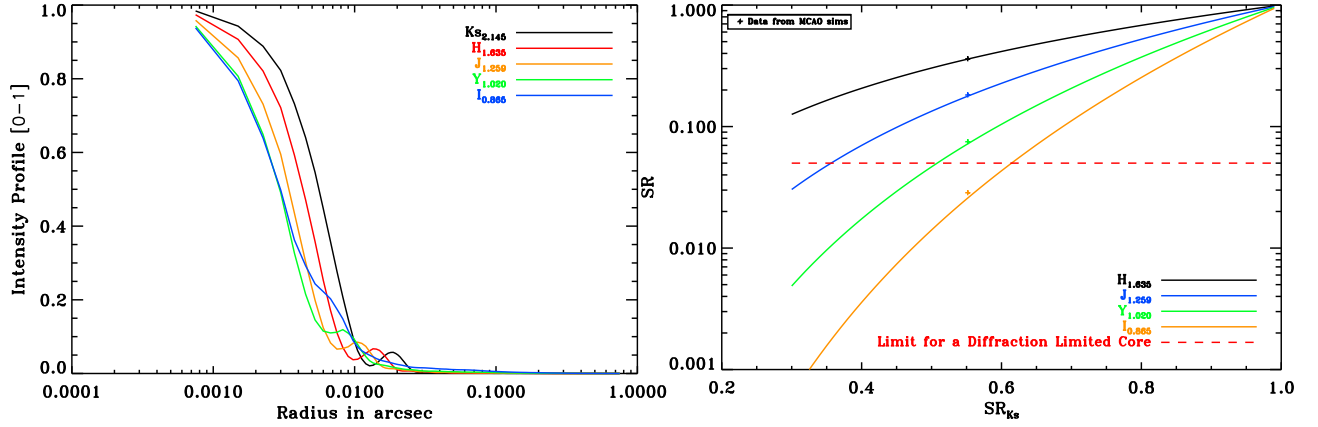


Figure 3. MCAO case: on the left panel the intensities profile. On the right the theoretical variation of the SR at I, Y, J, H vs SR in Ks, the "+" indicates the points we get from the simulations.

high Signal to Noise Ratio (SNR) point-like sources to compute star photometry by PSF fitting: combining the PSF of stars with different colors affects the model PSF, consequently the goodness of fit and the photometric errors are affected, especially for fainter stars.

3.1 Diffraction limited core

Despite of the fact that, at blue wavelengths, the nominal SR can be lower than what was previously expected,¹⁴ the central PSF core is almost diffraction limited also in the I band, see Figure 3 and Figure 4. See also Table 1. The small size of the core, also for the low SR case in I band, matches the left panel of Figure 3, where we see how the SR in I band almost superimpose to the theoretical curve derived from the Maréchal relation.¹⁵

Table 1. SR values for the star at the centre of the field. The error value is defined as the standard deviation across the different turbulence and aberration realizations. Here we give the values of the PSF realization used in the paper. It is the PSF expected at centre of the field. ρ and theta are the radius and the angle in radial coordinates.

ρ ["]	θ [deg]	SR I	SR Y	SR J	SR H	SR Ks
0.0	0.0	0.02 ± 0.01	0.07 ± 0.02	0.17 ± 0.04	0.35 ± 0.06	0.53 ± 0.05

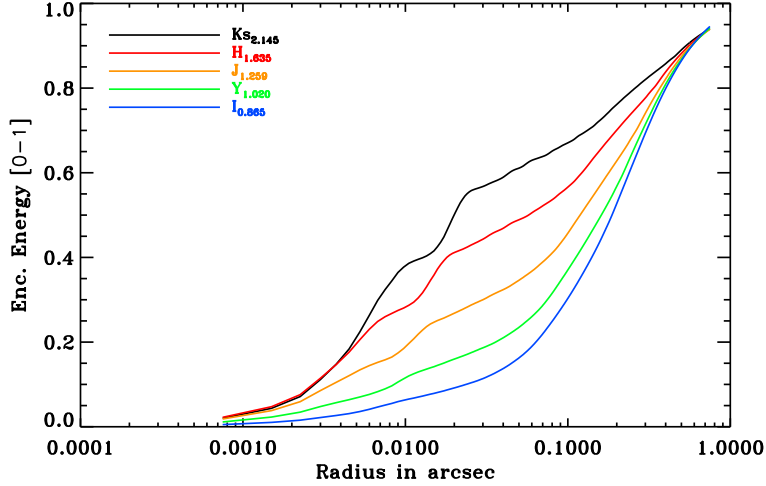
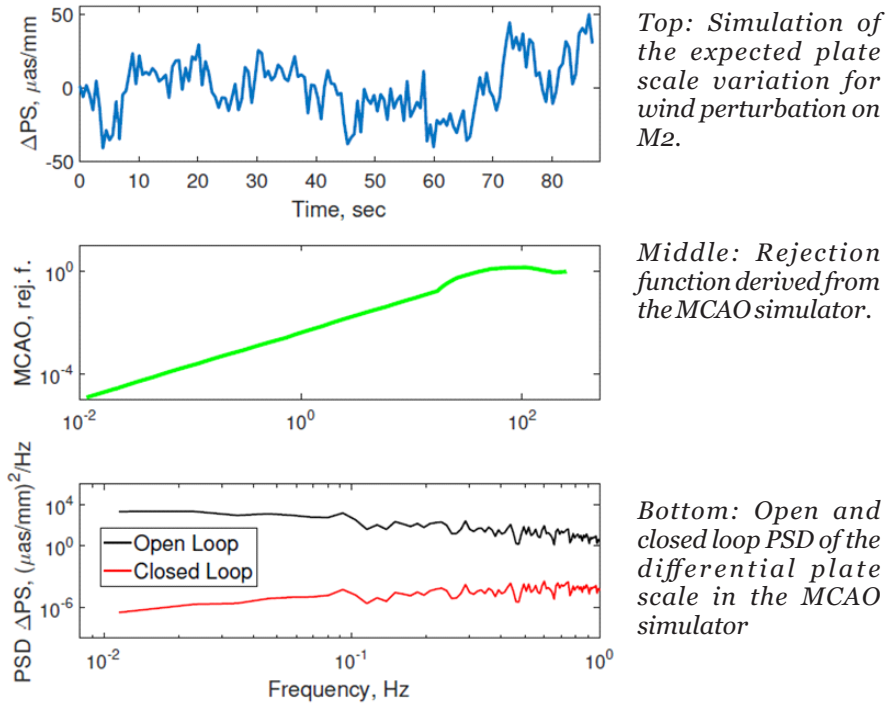


Figure 4. The figure shows the EE value for different radii.



Top: Simulation of the expected plate scale variation for wind perturbation on M2.

Middle: Rejection function derived from the MCAO simulator.

Bottom: Open and closed loop PSD of the differential plate scale in the MCAO simulator

Figure 5. The simulation indicates that the MCAO correction is able to fully stabilize the plate scale due to the axial positioning error of M2 originated from the wind perturbation.

4. ASTROMETRY

An important part of the SO WP activity is devoted to the characterization of the astrometric performance.^{16,17} We collaborate with the Astrometric Working Group (AWG) of MICADO in order to verify different aspects of the ELT-MICADO-MAORY system, as for example in Ref 18. In the context of the latter example, the analysis of the rejection function of the ELT plate scale performed by the MAORY MCAO was part of the study. See the Figure 5 showing the rejection function.

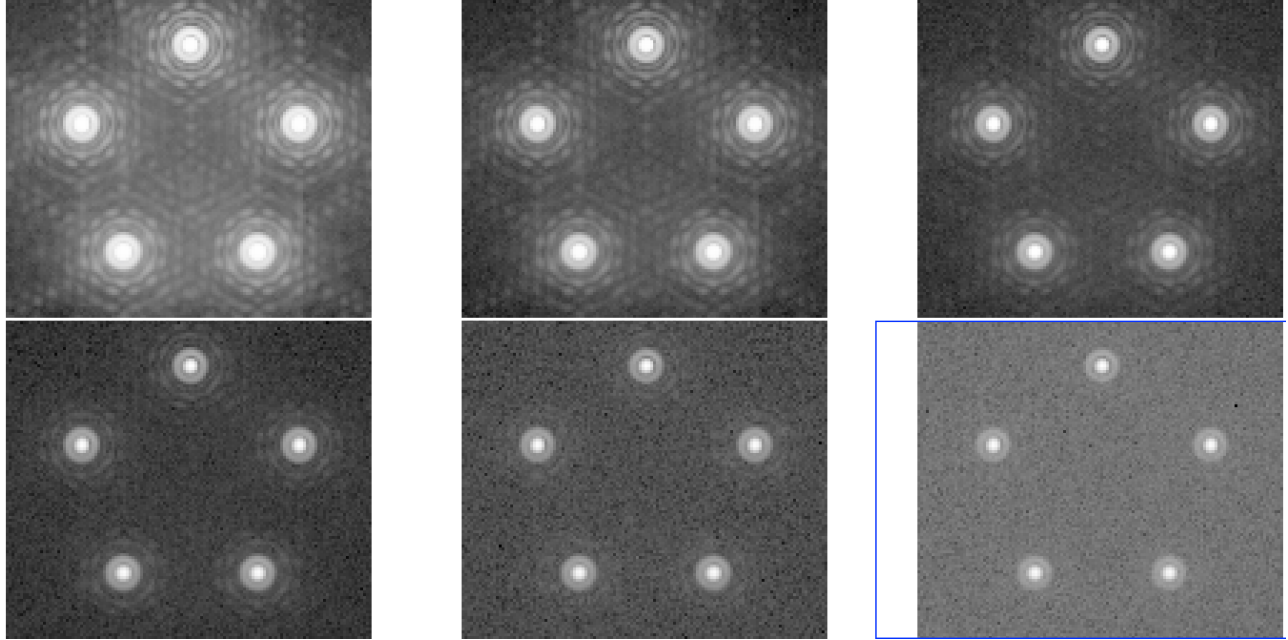


Figure 6. Log scale snapshots of the SimCADO simulations we ran to characterize the astrometric precision. The inset shows a constellation of five stars, realized for decreasing magnitude (brighter in the upper left, fainter in the lower right). The mag of stars the single stars in single plots 15th to 20th (H band).

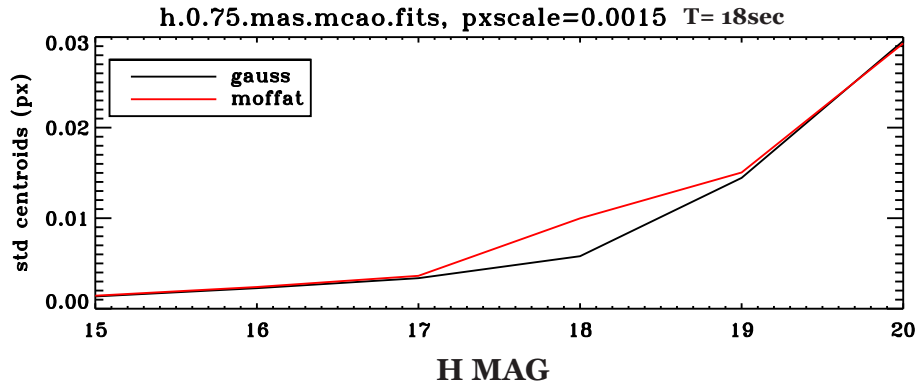


Figure 7. Squared sum of the centroid error standard deviation as measured on the data set simulated using SimCADO. Centroiding by PSF fitting using Moffat or Gauss functions.

4.1 Focal Plane Simulation for Astrometry

The two figures Figure 6 and Figure 7 give an example of simulations and results performed to characterize the astrometric precision. In particular here we focus on the basic centroid precision versus flux/magnitude, considering the MICADO pixel scale option of 1.5 mas/px. We used MCAO PSF and SimCADO¹⁹ to generate a number of simulated frames of the five star constellation for several magnitudes. In this way we want to derive the standard deviation of the centroid position of the stars, in H band and for different levels of flux. We simulated an exposure time of 18 seconds, and a constellation of 5 stars (same magnitudes). This $6s \times 3$ 18 seconds exposure corresponds to the total integrated time we get for the input PSF generated by PASSATA and MAO codes. For each magnitude bin, in the range from 15 to 20, we simulated ten frames. On each frame and for each star we accomplished the star center measurement by fitting a Gaussian or a Moffat²⁰ function. We have the tools to attack the astrometric problem in a End-2-End fashion. Using AETC or SimCADO, by the means of the MCAO PSF we generated, we can simulate focal plane images corresponding to our system in

different atmospheric and instrumental conditions.

5. LIMITING MAGNITUDE

Within the framework of the development of the science case for the characterization of massive star cluster formation in the high- z universe,²¹ we were interested to determine the available range of magnitude for detection of point sources. Since we are interested in the detection (see Figure 8) the noise in the SNR definition is the standard deviation of the sky far from bright objects. For sake of completeness, we extended the SNR definition toward a more photometric sense, adding the term due to the shot noise (with Poisson distribution) of the source. Here we considered the MICADO pixel scale option of 4.0 mas/px. We may compare this result with the one in Ref. 7 that states MICADO able to reach $H_{AB} = 30.8$ in 5 hours and SNR=5. The 0.3 difference may be due to a mismatch in the configuration of the telescope or MAORY+MICADO. However, it is small enough to avoid pushing for further analysis.

6. CONCLUSIONS

The SO WP takes advantage of the software developed by the MAORY technical team (as the PASSATA and MAO tools) to generate PSF models, the main ingredient to produce focal plane simulations. About the latter, the SO WP investigates in the direction of the identification and on the side of the testing of the tools for performance evaluation. The team is currently working on/with SimCADO and crosschecking with the Advanced Exposure Time Calculator²² (AETC). The Science Operation WG keeps updated the MAORY (and MICADO) instrument description by means of the PSF, the optical distortion, Quantum Efficiency and thermal background. In this way SO WG provides inputs to the MAORY Science Team, representing the bridge connecting it with the rest of MAORY group.

ACKNOWLEDGMENTS

The Science Operation Working Group members acknowledge the collaboration with the MICADO - MAORY working group for astrometry, the MAORY consortium, and the MAORY Science Team members.

REFERENCES

- [1] E. Diolaiti, “MAORY: A Multi-conjugate Adaptive Optics Relay for the E-ELT,” *The Messenger* **140**, 28–29 (2010).
- [2] G. Fiorentino, M. Bellazzini, P. Ciliegi, *et al.*, “Maory science cases white book,” (2017).
- [3] L. Schreiber, E. Diolaiti, M. Bellazzini, *et al.*, “Handling a highly structured and spatially variable Point Spread Function in AO images,” in *Second International Conference on Adaptive Optics for Extremely Large Telescopes. Online at $\url{http://ao4elt2.lesia.obspm.fr}$ $\&$ $\url{http://ao4elt2.lesia.obspm.fr/j/A}$* , P57 (2011).
- [4] P. Ciliegi, E. Diolaiti, M. Bellazzini, *et al.*, “Organization, management and risk analysis of the MAORY project,” in *Modeling, Systems Engineering, and Project Management for Astronomy VIII*, G. Z. Angeli and P. Dierickx, Eds., **10705**, 581 – 587, International Society for Optics and Photonics, SPIE (2018).
- [5] J. M. Beckers, “Increasing the size of the isoplanatic patch with multiconjugate adaptive optics,” in *ESO Conference on Very Large Telescopes and their Instrumentation*, **2**, 693–703 (1988).
- [6] J. M. Beckers, “Detailed compensation of atmospheric seeing using multiconjugate adaptive optics,” in *Active Telescope Systems, Proc. SPIE* **1114**, 215–217 (1989).
- [7] R. Davies, N. Ageorges, L. Barl, *et al.*, “MICADO: the E-ELT adaptive optics imaging camera,” in *Proc. SPIE, Society of Photo-Optical Instrumentation Engineers (SPIE) Conference Series* **7735**, 77352A (2010).
- [8] C. Arcidiacono, L. Schreiber, G. Bregoli, *et al.*, “End to end numerical simulations of the MAORY multi-conjugate adaptive optics system,” in *Adaptive Optics Systems IV*, *Proc. SPIE* **9148**, 91486F (2014).
- [9] R. Ragazzoni, “Pupil plane wavefront sensing with an oscillating prism,” *Journal of Modern Optics* **43**, 289–293 (1996).

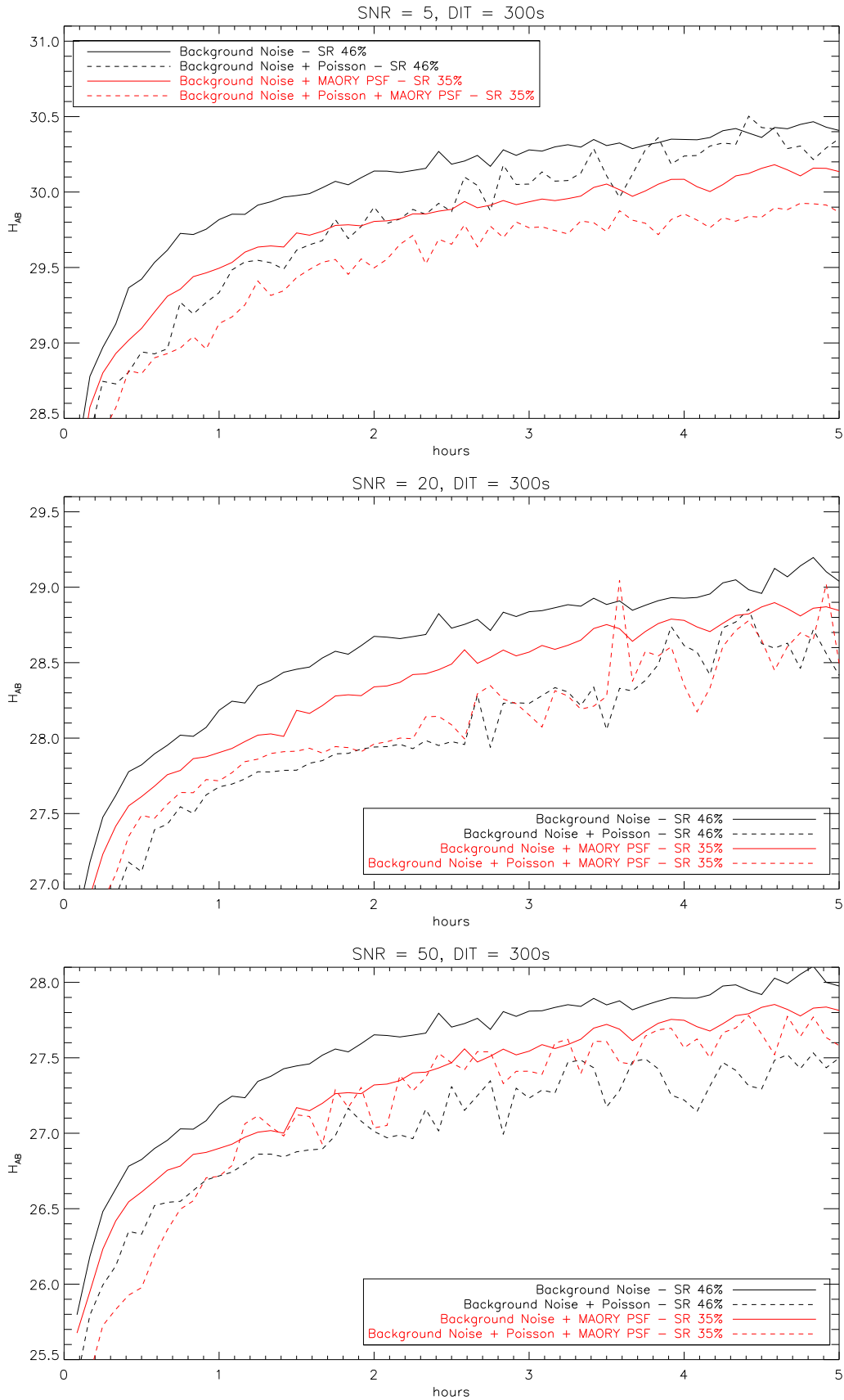


Figure 8. AB H limiting magnitude for different SNR level, with and without object photon noise and for two different SR values.

- [10] G. Agapito, A. Puglisi, and S. Esposito, “PASSATA: object oriented numerical simulation software for adaptive optics,” in *Adaptive Optics Systems V*, E. Marchetti, L. M. Close, and J.-P. Vran, Eds., **9909**, 2164 – 2172, International Society for Optics and Photonics, SPIE (2016).
- [11] D. Gratadour, E. Gendron, and G. Rousset, “Intrinsic limitations of shack–hartmann wavefront sensing on an extended laser guide source,” *J. Opt. Soc. Am. A* **27**, A171–A181 (2010).
- [12] J. von Neumann and R. D. Richtmyer, “Statistical Methods in Neutron Diffusion,” tech. rep., LAMS (1947).
- [13] P. B. Stetson, “DAOPHOT: A Computer Program for Crowded-Field Stellar Photometry,” *PASP* **99**, 191 (1987).
- [14] E. Diolaiti, J.-M. Conan, I. Foppiani, *et al.*, “Towards the phase A review of MAORY, the multi-conjugate adaptive optics module for the E-ELT,” in *Adaptive Optics for Extremely Large Telescopes*, 02007 (2010).
- [15] A. Maréchal, “Étude des effets combinés de la diffraction et des aberrations géométriques sur l’image d’un point lumineux,” *Rev. Opt. Theor. Instrum.* **26**, 257–277 (1947).
- [16] S. Trippe, R. Davies, F. Eisenhauer, *et al.*, “High-precision astrometry with MICADO at the European Extremely Large Telescope,” *MNRAS* **402**, 1126–1140 (2010).
- [17] M. Patti, C. Arcidiacono, M. Lombini, *et al.*, “The impact of geometric distortions in multiconjugate adaptive optics astrometric observations with future extremely large telescopes,” *MNRAS* **487**, 1140–1148 (2019).
- [18] G. Rodeghiero, J. U. Pott, C. Arcidiacono, *et al.*, “The impact of ELT distortions and instabilities on future astrometric observations,” *MNRAS* **479**, 1974–1985 (2018).
- [19] K. Leschinski, O. Czoske, R. Khler, *et al.*, “SimCADO: an instrument data simulator package for MICADO at the E-ELT,” in *Modeling, Systems Engineering, and Project Management for Astronomy VI*, G. Z. Angeli and P. Dierickx, Eds., **9911**, 777 – 793, International Society for Optics and Photonics, SPIE (2016).
- [20] A. F. J. Moffat, “A Theoretical Investigation of Focal Stellar Images in the Photographic Emulsion and Application to Photographic Photometry,” *A&A* **3**, 455–461 (1969).
- [21] E. Vanzella, F. Calura, M. Meneghetti, *et al.*, “Massive star cluster formation under the microscope at $z = 6$,” *MNRAS* **483**, 3618–3635 (2019).
- [22] R. Falomo, D. Fantinel, and M. Uslenghi, “AETC: Advanced Exposure Time Calculator,” in *Proc. SPIE, Society of Photo-Optical Instrumentation Engineers (SPIE) Conference Series* **8135**, 813523 (2011).